

Critical jamming of frictional grains in the generalized isostaticity picture

Silke Henkes,¹ Martin van Hecke,² and Wim van Saarloos¹

¹*Instituut-Lorentz, LION, Leiden University, P.O. Box 9506, 2300 RA Leiden, Netherlands*

²*Kamerlingh Onnes Laboratory, LION, Leiden University, P.O. Box 9504, 2300 RA Leiden, Netherlands*

While frictionless spheres at jamming are isostatic, frictional spheres at jamming are not. As a result, frictional spheres near jamming do not necessarily exhibit an excess of soft modes. However, a generalized form of isostaticity can be introduced if fully mobilized contacts at the Coulomb friction threshold are considered as slipping contacts. We show here that, in this framework, the vibrational density of states (DOS) of frictional discs exhibits a plateau when the generalized isostaticity line is approached. The crossover frequency ω^* scales linearly with the distance from this line. Moreover, we show that the frictionless limit $\mu \rightarrow 0$, which appears singular when fully mobilized contacts are treated elastically, becomes smooth when fully mobilized contacts are allowed to slip.

PACS numbers: 45.70.-n, 46.55.+d, 63.50.-x, 81.05.Rm

The jamming transition in disordered media has been the focus of intensive research efforts in recent years. For frictionless spheres, the transition occurs at the isostatic point where the contact number z reaches $z_{\text{iso}}^0 = 2d$ [1]. This point, known as point J, acts as a critical point: close to it the spectrum of vibrational modes shows an excess density of states (DOS) at low frequencies, with a finite number of zero-energy modes at the jamming transition and a cross-over frequency $\omega^* \sim (z - z_{\text{iso}}^0)$ [2, 3].

Friction has to be introduced to make connection with the granular systems studied in experiments [4], in engineering [5] and in the geosciences [6]. For frictional spheres, the contact number at the transition lies in the range $z_{\text{iso}}^{\mu} = d + 1 \leq z \leq 2d$, depending on the preparation method and the friction coefficient μ of the material. The frictional isostatic value z_{iso}^{μ} derives from a counting argument assuming *arbitrary* tangential friction forces, and is reached in practice at jamming in the limit $\mu \rightarrow \infty$, for gently prepared packings [7, 8, 9].

However, the magnitude of the tangential forces is limited by the Coulomb criterion $|f_t| \leq \mu f_n$. Let $m = |f_t|/\mu f_n$ be the mobilization of a contact, such that contacts at the Coulomb threshold, so-called fully mobilized contacts, have $m = 1$. Crucially, there can be a finite fraction of contacts at the mobilization threshold, i.e. with fixed ratio $|f_t|/\mu f_n$ [10, 11]. This affects the counting arguments, and suggests to consider a generalized isostaticity condition [7].

We define $n_m \in [0, z/2]$ as the fraction of contacts per particle at the Coulomb threshold. For frictional particles, the tangential forces introduce $d - 1$ additional force components at each contact. Then for a packing to be stable, the $Nd(d + 1)/2$ rotational and translational degrees of freedom need to be constrained by the $Nzd/2 - Nn_m$ independent force components. This lead Shundyak *et al.* [7] to propose the *generalized isostaticity* criterion

$$z \geq (d + 1) + \frac{2n_m}{d} \equiv z_{\text{iso}}^m. \quad (1)$$

Simulations have shown that as frictional packings are

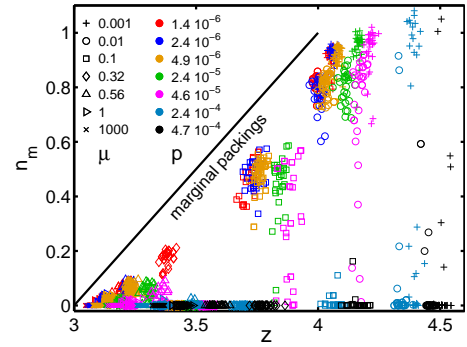


FIG. 1: Position of our packing configurations in the phase space defined by z and n_m in our $2d$ simulations. The generalized isostaticity line $n_m = d(z - z_{\text{iso}}^m)/2 = z - 3$ is shown in black. Stable packings can not exist left of this line. Each marker denotes one of 30 configurations at a given (μ, p) with the color-marker combinations indicated by the legend. For a given μ (a given symbol), configurations with larger p are to the right, and n_m drops to zero for the largest pressures.

prepared gently, the fraction of fully mobilized contacts at jamming indeed is such that z approaches the generalized isostaticity line $z = z_{\text{iso}}^m$ in the z - n_m plane (Fig. 1), in accord with an earlier suggestion by Bouchaud [10].

Fully mobilized contacts can not resist tangential perturbations, and simulations evidence that a substantial part of the movement of frictional piles is due to contacts failing at the mobilization threshold [5, 11, 12, 13]. The exact values of n_m for $0 < \mu < \infty$ depend on the preparation method [9, 12], but in the limit of very “gentle” equilibration so as to approach the jamming threshold, they are a smooth decreasing function of μ [7, 8, 9]. For $2d$ systems, one finds that $n_m \rightarrow 1$ in the frictionless limit since $z \approx z_{\text{iso}}^0 = 4$, while $n_m \rightarrow 0$ in the limit $\mu \rightarrow \infty$, as z then approaches the frictional isostaticity criterion $z = d + 1$.

In this paper, we show that the similarities between frictionless and frictional static sphere packings, which are brought to the foreground by this concept of general-

ized isostaticity, also extend to the dynamic properties. We do so by calculating the density of states (DOS) of frictional sphere packings, while taking into account that contacts at the mobilization threshold $m = 1$ slip with unchanged tangential forces during small amplitude vibrations. We recover the low-frequency plateau in the DOS which is characteristic for packings of frictionless particles near jamming. We find that the rescaled crossover frequency $\tilde{\omega}^* = \omega^*/p^{1/6}$ scales linearly with the distance from the generalized isostaticity line, as $\tilde{\omega}^* \sim (z - z_{\text{iso}}^m)$, see Fig. 2a. An analysis of the eigenmodes shows that the dominant low-energy displacements consist of particles rolling without sliding for contacts with $m \neq 1$, and tangential sliding at contacts with $m = 1$.

This scenario nicely generalizes the findings for frictionless spheres to the frictional case. Our findings stress the crucial role of the response of fully mobilized contacts. When instead, these are all taken to be elastic, the inclusion of friction becomes a singular perturbation, and the excess low-frequency modes seen in frictionless packings are suppressed [14].

Simulation method — We perform a numerical analysis of two-dimensional packings of frictional particles interacting with Hertz-Mindlin forces (during the preparation of the packings, energy is dissipated through viscous damping — see [7, 14]). The Hertz-Mindlin interaction is comprised of a normal interaction that scales as $\delta^{3/2}$, where δ is the overlap of the particles, and an incremental tangential interaction which is limited by the Coulomb criterion $f_t \leq \mu f_n$ [15]. The packings are made at fixed friction coefficient μ and pressure p .

Motivated by (1), we map the configurations in the phase space of Fig. 1 spanned by z and n_m . The generalized isostaticity criterion $z = z_{\text{iso}}^m$ then defines a *line of marginal packings* with end points ($z = 3, n_m = 0$) and ($z = 4, n_m = 1$), so that stable packings lie to the right of it. As in [7], we observe that for sufficiently gentle preparation methods, packings approach the generalized isostaticity line in the limit $p \rightarrow 0$. Hence we identify this line with the (zero pressure) jamming transition for slowly equilibrated frictional discs. For larger pressures, packings attain higher contact numbers, and we find a range of pressures where the distribution of n_m is bimodal (see e.g. the configurations for ($\mu = 0.001, p = 2.4 \cdot 10^{-4}$), due to the interplay of elastic and viscous forces during the preparation of the packings [9]. We focus here on the behavior for $p \rightarrow 0$ at fixed viscous damping.

Treatment of small amplitude vibrations — The vibrational density of states is obtained by linearizing the equations of motion around each stable state. Rattlers, which give rise to trival zero-frequency modes, are left out from the analysis from the start.

There are several subtleties associated with frictional response. First of all, the nature of the ideal Coulomb condition $|f_t| \leq \mu f_n$ implies a discontinuous response for sliding displacements at fully mobilized contacts. For

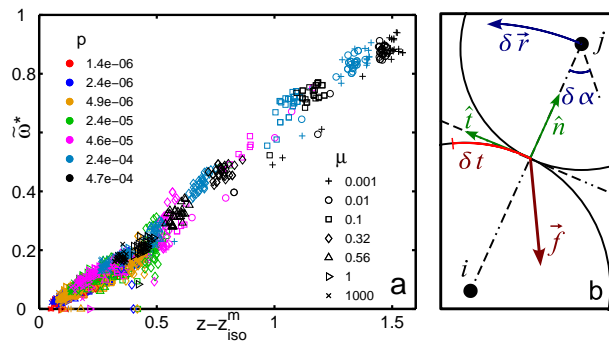


FIG. 2: (a) Normalized crossover frequency $\tilde{\omega}^*$ where the plateau in the DOS is reached as a function of the distance $z - (3 + n_m)$ from the line of generalized isostaticity. The relation is linear, in spite of the change of the μ - n_m -relation at larger pressures (see Fig. 1). (b) Contact geometry illustrating the various displacements and rotations as well as the effective tangential displacement $\delta \vec{t}$ of the contact point. For simplicity, we have assumed that particle i is stationary.

displacements which lead to an increase in the tangential force f_t (taking f_n fixed), the Coulomb condition then implies that the contact slips with f_t unchanged — this translates into a contact stiffness $k_t = 0$ for this displacement. For displacements in the opposite direction, however, f_t will decrease so that k_t is effectively nonzero!

This separation into two types of displacements at fully mobilized contacts is only meaningful for static response studies. Under vibrations, modes effectively couple through the Coulomb condition; moreover fully mobilized contacts dissipate energy during the slipping half of the phase, and a decomposition into purely nondissipative eigenmodes is not possible. In order to avoid these complications — which are artifacts of the singular nature of the ideal Coulomb condition — we here simply put the tangential stiffness $k_t = 0$ for all fully mobilized contacts: *fully mobilized contacts are treated as slipping contacts in both directions*. This allows us to study the DOS of these modes.

Secondly, a detailed analysis of the dynamics shows that there always is, even at contacts which are not fully mobilized, a nonpotential term in the dynamical equations due to the tangential friction [9]. The origin of this term is the change in the direction of the tangential friction force when a contact point rolls over a particle. This effect is of the order of f_t itself, which for our Mindlin forces scales as $\sim \delta^{3/2}$. Hence for packings close to jamming, the contribution of these terms can be neglected in comparison with the normal and tangential springs which scale as $\delta^{1/2}$; for this reason we will disregard these terms in our analysis below (similar to what is often done with the pre-stress terms in frictionless packings).

With these approximations, the equations of motion are conservative to first order, and their structure resembles what one finds for the vibrational properties of

frictionless particles. After we expand the equation of motion around the equilibrium we obtain equations of motion of the form $\delta\ddot{r}_\alpha = -D_{\alpha\beta}\delta r_\beta + O(\delta r^2)$, where the dynamical matrix $D_{\alpha\beta}$ can, with the present simplifications and after a rescaling of the coordinates by the square root of the masses/moments of inertia, be written in terms of the derivatives of an effective potential, $D_{\alpha\beta} = (m_\alpha m_\beta)^{-1/2} \frac{\partial^2 V}{\partial \delta r_\alpha \partial r_\beta}$ [9]. For our packings with Hertz-Mindlin forces the effective potential is given by

$$V = \frac{1}{2} \sum_{\langle ij \rangle} k_n (\delta \vec{r} \cdot \hat{n})^2 - \frac{f_n}{r^0} (\delta \vec{r} \cdot \hat{t})^2 + k_t \delta t^2, \quad (2)$$

where $\delta t = (\delta \vec{r} \cdot \hat{t}) - (R_i \delta \alpha_i + R_j \delta \alpha_j)$ is the tangential displacement of the contact point of the two particles, as illustrated in Fig. 2(b). Here k_n and k_t are the normal and tangential stiffness, respectively, which derive from the Hertz-Mindlin interaction law and which both scale as $k \sim \delta^{1/2}$ [15, 16]. In this formulation, the vibrational spectrum is a histogram of the eigenvalues ω_k^2 of $D_{\alpha\beta}$ as a function of the associated frequencies ω_k .

Density of States — We have studied the vibrational density of states (DOS) for a wide range of friction coefficients ($\mu \in [10^{-3}, 10^3]$) and pressures ($p \in [10^{-6}, 10^{-3}]$). As in previous work [14], we plot the density of states as a function of the rescaled frequencies $\tilde{\omega} = \omega/p^{1/6}$, appropriate for Hertz-Mindlin forces which exhibit a trivial softening with frequencies scaling as $\sqrt{k} \sim p^{1/6}$.

Figs. 3a-b show the DOS for the smallest pressure ($p = 1.41 \cdot 10^{-6}$), i.e, close to the generalized isostaticity line, for the full range of μ . When the fully mobilized contacts are allowed to slip, the density of states clearly shows an excess number of low-energy modes (Fig. 3a). Otherwise, when all contacts are chosen to have a finite k_t , the plateau in the DOS disappears for small friction coefficients, where n_m is large (Fig. 3b and [14]).

In Fig. 3c, we show the evolution of the density of states, again allowing fully mobilized contacts to slip, with increasing pressure for $\mu = 0.3$. The low-frequency part of the DOS shows linear $D(\tilde{\omega}) \sim \tilde{\omega}$ Debye-like behavior up to a normalized frequency $\tilde{\omega}^*$ which increases with pressure. In the frictionless case, $\tilde{\omega}^*$ marks the frequency scale below which the packing can be treated like an elastic solid and above which the DOS shows a plateau [3]. For our frictional packings, an extension of this argument then predicts the scaling $\tilde{\omega}^* \sim z - z_{\text{iso}}^m$ with in $2d$ the generalized isostatic contact number $z_{\text{iso}}^m = 3 + n_m$ — we will verify this prediction below.

We extract $\tilde{\omega}^*$ in the following way: Since the DOS at different pressures do not have similar functional forms, we cannot rescale the integrated DOS as was done in [14]. Instead, we smooth the integrated DOS to obtain an interpolated DOS. Then $\tilde{\omega}^*$ is determined by the point at which $D(\tilde{\omega})$ reaches a value of 0.2, normalized to the height of the plateau at $\tilde{\omega} = 1$, to avoid nonlinearities in the approach to the plateau. Fig. 2a shows the $\tilde{\omega}^*$ we

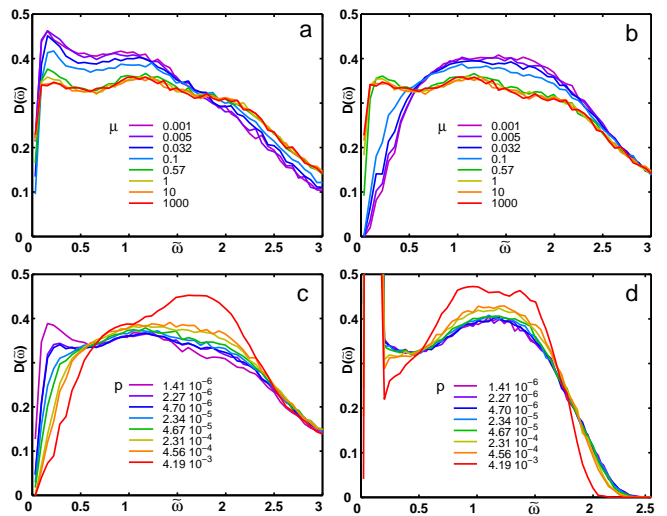


FIG. 3: Density of states (DOS). (a) DOS with fully mobilized contacts treated as slipping for the smallest pressure $p = 1.41 \cdot 10^{-6}$ (approaching the line of generalized isostaticity) for a range of μ . (b) DOS for the same packings as in (a), but with all contacts treated as non-slipping, as in [14]. (c) Illustration of the low frequency plateau developing in the DOS as p is decreased, for an intermediate friction coefficient $\mu = 0.3$ and with $m = 1$ -contacts slipping. (d) DOS for range of pressures and $\mu = 0.001$, with the tangential stiffness constant set to $k_t^{1/2} = 0.04 k_n^{1/2}$ (see text).

obtain for different μ and p as a function of $z - z_{\text{iso}}^m$. The relation is linear to a good approximation, confirming our prediction.

Even if the fully mobilized contacts are allowed to slip, the density of states for $\mu \rightarrow 0$ is still noticeably different from the frictionless case with $\mu = 0$ (although both have an excess of low-density modes). This is because the non-mobilized contacts still have a finite tangential stiffness k_t comparable to the stiffness for compression of bonds k_n , and hence a finite influence — this is even true when p approaches zero and the system approaches generalized isostaticity. Clearly, this non-smooth behavior has its root in the singular change of the dynamical matrix, due to the finite value of k_t of many contacts [14]. Fig. 3d illustrates that when one takes the limit $k_t \rightarrow 0$ in the dynamical matrix, one recovers the frictionless DOS, with a δ -function of weight N due to trivial rotational modes at $\tilde{\omega} = 0$ [17].

Nature of the low-energy displacements — We now investigate the nature of the eigenmodes of the low-energy eigenvalues of the dynamical matrix. Eq. (2) predicts the nature of the lowest-energy displacements in the limit $\tilde{\omega} \rightarrow 0$, $p \rightarrow 0$. The prefactors of the tangential, normal and sliding displacements scale as $\delta^{3/2}$, $\delta^{1/2}$ and $\delta^{1/2}$, respectively, for a contact with $m \neq 1$. For a $m = 1$ -contact, $k_t = 0$. Therefore, in the limit discussed above, the only low-energy displacement allowed for $m \neq 1$ is a purely tangential motion in combination with rotations of the

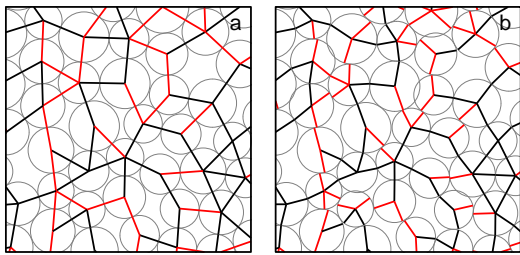


FIG. 4: Sample displacement for a low-energy eigenvector at $p = 1.41 \cdot 10^{-6}$ and $\mu = 0.001$. (a) Contact network in the initial state, with fully mobilized contacts in red. (b) Particles have been displaced proportional to the mode amplitude. The lines now link the particle centers to the position of the former contact points after rotation. If $\delta t \neq 0$, the contact line between particles is broken.

particles in such a way that there is no tangential sliding. For $m = 1$ contacts, the movement still has to be tangential, but sliding at the contact is permitted. A simple illustration of the displacements in a low-energy, low p mode is shown in Fig. 4: the difference in the rotational response between slipping fully mobilized contacts and non-slipping non-mobilized contacts is clearly visible.

The occurrence of floppy modes at generalized isostaticity, and their spatial structure which locally exhibits rolling and sliding depending on the contacts mobilization, can be understood from a counting argument. The $3N$ degrees of freedom of the packing participating in a floppy deformation need to satisfy two groups of constraints: setting the normal motion at each contact to zero gives $Nz/2$ constraints, while setting the sliding motion at each $m \neq 1$ -contact to zero gives $Nz/2 - Nn_m$ constraints. Hence the number of constraints of the motion is exactly equal to the number of degrees of freedom only if $z = z_{\text{iso}}^m = 3 + n_m$ — floppy modes arise at generalized isostaticity. Note that the variational argument of Wyart *et al.* [3] that estimates $\tilde{\omega}^*$ in terms of distorted floppy modes then generalizes in our case to $\tilde{\omega}^* \sim z - z_{\text{iso}}^m$.

In the limit $\mu \rightarrow 0$, we observe that $n_m \rightarrow 1$ (every other contact is fully mobilized, see also [7]), so that at that point on the generalized isostaticity line, the $Nz/2 - Nn_m = N$ contacts with $m \neq 1$ equal precisely the number of rotational degrees of freedoms. Hence there are precisely enough contacts to couple the rotations to the translations. Unlike in the case of the spherical limit of ellipsoids, where the rotational modes appear in the gap of translational modes [17, 18], here translations and rotations remain strongly coupled.

Conclusion and outlook — The jamming transition of frictional packing of spheres is more complex than the transition at point J for frictionless spheres. However, we show that along the *generalized isostatic line* in the space spanned by the contact number z and the number of fully mobilized contacts n_m , the system shows crit-

ical behavior similar to the frictionless case if slipping contacts at $m = 1$ are incorporated into the dynamical matrix. In this case, the DOS shows a plateau near the z_{iso}^m -line, and at larger pressure, the crossover frequency scales as $\tilde{\omega}^* \sim (z - z_{\text{iso}}^m)$.

The relation between the friction coefficient and n_m is poorly understood except for the limiting cases $\mu \rightarrow \infty$ and $\mu \rightarrow 0$. Our simulations indicate that this relation depends significantly on the preparation method of the sample, where packings prepared with higher viscous damping have larger n_m [9]. The z - n_m phase diagram can be a tool to understand the behavior of more complex packings. For example, for a packing undergoing an avalanche, the number of fully mobilized contacts increases before the system rearranges, so that the system moves along a vertical path in the z - n_m space which eventually crosses the z_{iso}^m -line [12].

Acknowledgement — We are grateful to K. Shundyak for help and use of his packings. SH gratefully acknowledges support from the physics foundation FOM.

-
- [1] C. S. O'Hern, L. E. Silbert, A. J. Liu, and S. R. Nagel, Phys. Rev. E **68**, 011306 (2003).
 - [2] L. E. Silbert, A. J. Liu, and S. R. Nagel, Phys. Rev. Lett. **95**, 098301 (2005).
 - [3] M. Wyart, L. E. Silbert, S. R. Nagel, and T. A. Witten, Phys. Rev. E **72**, 051306 (2005).
 - [4] T. S. Majmudar and R. P. Behringer, Nature **435**, 1079 (2005).
 - [5] S. J. Antony and N. P. Kruyt, Phys. Rev. E **79**, 031308 (2009).
 - [6] J. L. Anthony and C. Marone, J. Geophys. Res. **110** (2005).
 - [7] K. Shundyak, M. van Hecke, and W. van Saarloos, Phys. Rev. E **75**, 010301 (R) (2007).
 - [8] H. P. Zhang and H. A. Makse, Phys. Rev. E **72**, 011301 (2005).
 - [9] S. Henkes, K. Shundyak, M. van Hecke, and W. van Saarloos, in preparation.
 - [10] J.-P. Bouchaud, in *Les Houches Session LXXXVII*, edited by J.-L. Barrat, M. Feigelman, J. Kurchan, and J. Dalibard (Springer, Heidelberg, 2004).
 - [11] L. E. Silbert, D. Ertaş, G. S. Grest, T. C. Halsey, and D. Levine, Phys. Rev. E **65**, 051307 (2002).
 - [12] S. Deboeuf, O. Dauchot, L. Staron, A. Mangeney, and J.-P. Vilotte, Phys. Rev. E **72**, 051305 (2005).
 - [13] M. Wyart, EPL **85**, 24003 (2009).
 - [14] E. Somfai, M. van Hecke, W. G. Ellenbroek, K. Shundyak, and W. van Saarloos, Phys. Rev. E **75**, 020301 (R) (2007).
 - [15] K. L. Johnson, *Contact Mechanics* (Cambridge University Press, 1985).
 - [16] E. Somfai, J.-N. Roux, J. H. Snoeijer, M. van Hecke, and W. van Saarloos, Phys. Rev. E **72**, 021301 (2005).
 - [17] Z. Zeravcic, N. Xu, A. J. Liu, S. R. Nagel, and W. van Saarloos, to appear in EPL, arXiv:0904.1558.
 - [18] M. Mailman, C. F. Schreck, C. S. O'Hern, and B. Chakraborty, Phys. Rev. Lett **102**, 255501 (2009).